Mechanism of Metal Oxide Nanoparticle Loading in SBA-15 by the Double Solvent Technique

ARTICLE *in* THE JOURNAL OF PHYSICAL CHEMISTRY C · FEBRUARY 2010

Impact Factor: 4.77 · DOI: 10.1021/jp907002y

6 AUTHORS, INCLUDING:

Juliette van der Meer
Bruker Daltronics
3 PUBLICATIONS **80** CITATIONS
SEE PROFILE

Isabelle Bardez-Giboire
Atomic Energy and Alternative Energies Co…
24 PUBLICATIONS **197** CITATIONS
SEE PROFILE

Cyrille Mercier
University of Valenciennes and Hainaut-Ca…
25 PUBLICATIONS **179** CITATIONS
SEE PROFILE

Anne Davidson
Pierre and Marie Curie University - Paris 6
72 PUBLICATIONS **1,991** CITATIONS
SEE PROFILE

Mechanism of Metal Oxide Nanoparticle Loading in SBA-15 by the Double Solvent Technique

Juliette van der Meer,[†,‡] Isabelle Bardez-Giboire,[‡] Cyrille Mercier,[§] Bertrand Revel,[||] Anne Davidson,[⊥] and Renaud Denoyel*[,#]

CNRS-ICSM UMR 5257, Bagnols-sur-Cèze, France, CEA, DEN, DTCD/SECM/LDMC, F-30207 Bagnols-sur-Cèze, France, Laboratoire des Matériaux et Procédés (LMP), Université de Valenciennes et du Hainaut-Cambrésis, Valenciennes, France, Centre Commun de Mesure de RMN, Université des Sciences et Technologies Lille 1, Villeneuve d'Ascq, France, Laboratoire de Réactivité de Surface-UMR, Université Paris 6, Paris, France, and Laboratoire Chimie Provence-UMR 6264, Université de Provence, Marseille, France

Received: July 23, 2009; Revised Manuscript Received: January 14, 2010

The interaction between SBA-15 mesoporous silica, alkane solvents, and water has been studied to understand the mechanism of the so-called double solvent technique. This method facilitates the loading of the pores of SBA-15 with a metal oxide precursor solution, by prewetting the SBA-15 with an alkane. In a previous study on cobalt oxide, it has been observed that differences in particle size, shape, and dispersion were obtained as a function of the solvent used (*n*-pentane, *n*-hexane, *n*-heptane, and cyclohexane). In order to understand this phenomenon and to explain the differences between the effects that the alkane solvents exert, a combined FT-IR spectroscopy, solid state NMR spectroscopy, and microcalorimetry study has been carried out. Though subtle, interactions between alkanes and the silica surface are different, indicating a more pronounced modification of the surface, i.e., rehydroxylation, in the presence of pentane. It is suggested that this leads to a better wettability and therefore increases the introduction of aqueous solutions into the pores. Moreover, the lower vapor pressure of this component, its lower interaction energy with the surface, and its lower interfacial tension toward water enhance the dispersion of the metal oxide precursor inside the pore network.

Introduction

Since its discovery in 1998 by the team of Zhao, Stucky, et al.,[1] a large number of studies have been dedicated to SBA-15 mesoporous silica. Its characteristics, such as the tunable pore size, narrow pore size distribution, large specific surface area, and relative stability in water, make this material very attractive for many applications, such as catalysis,[2−4] biosensing,[5,6] and controlled drug release.[7,8] We have taken SBA-15 as a model to test whether it is possible to condition chloride waste by nanotrapping. Radioactive chloride salt results from the pyrochemical treatment of spent nuclear fuel of Generation IV reactors.[9] This type of waste is rich in chlorine, alkali, and alkaline earth elements, which makes it hard to vitrify, since a glass matrix will leach. Solutions are sought in the conditioning in a crystalline form as a ceramic. Another idea that was launched is to immobilize the waste, trapped in the nanopores of a durable matrix. For this application, analogues were sought in the catalysis chemistry domain. A way to obtain nanoparticles, which have manifold applications in catalysis, is to mold them in the pores of a support. To do so, a common method to fill the pores is by impregnating them with a salt solution of the precursors of the desired metals or oxides, a process that could possibly be applied with radioactive chloride solutions as well.

Several studies have been dedicated to SBA-15 silica as a support for nanoparticles of manganese and cobalt oxide.[10,11] As precursors, salt solutions of metal nitrates are used. A problem is the bad dispersion when impregnating the SBA-15 directly with the solution.[12] Different methods have been reported to obtain homogeneously dispersed nanoparticles.[13−15] One of the techniques to improve the dispersion is the double solvent technique, developed by Lopes et al.[12] The surface of the SBA-15, which is in powder form, is prewetted by *n*-hexane, before an aqueous solution of the desired precursor is added. This results in a significantly better dispersion of the cobalt oxide nanoparticles, obtained after drying and calcination. A study to compare the influence on the particle dispersion using other alkane solvents has been carried out.[16] For this purpose, in addition to *n*-hexane, also *n*-pentane, *n*-heptane, and cyclohexane were used, also for reasons of decreasing the toxicity compared to working with *n*-hexane. An important observation made was that the dispersion and size of the cobalt oxide nanoparticles differed as a function of the solvent used. The use of pentane in the prewetting stage gave rise to finely dispersed, small nanoaggregates, whereas when cyclohexane was used, large, unevenly distributed aggregates were obtained. Therefore the question arose: what are the mechanisms of the double solvent technique and what causes the difference between the solvents?

Some properties, found in literature, of the alkane solvents we have studied are noted here. To understand the behavior of the system "mesoporous silica−solvent−water", several parameters need to be taken into account. The interfacial tension between alkanes and water is 48.7 $mN \cdot m^{-1}$ [17] for pentane, which is smaller than the other three solvents that have been studied: 50.4, 50.7 $mN \cdot m^{-1}$ for, respectively, hexane and heptane[18] and 50.3 $mN \cdot m^{-1}$ for cyclohexane,[19] all measured at 298 K. This

* To whom correspondence should be addressed. E-mail: renaud.denoyel@univ-provence.fr.
[†] CNRS-ICSM UMR 5257.
[‡] DTCD/SECM/LDMC.
[§] Université de Valenciennes et du Hainaut-Cambrésis.
[||] Université des Sciences et Technologies Lille 1.
[⊥] Université Paris 6.
[#] Université de Provence.

10.1021/jp907002y
Published on Web 02/05/2010

would imply that smaller droplets of water or an aqueous solution are easier to be formed in pentane, rather than in hexane, heptane, or cyclohexane. This could possibly result in the formation of smaller nanoparticles in the case of pentane. Further, literature research has been carried out on the enthalpy of adsorption of alkane solvents onto the silica surface. Values have not been found for SBA-15; however, some have been measured for a porous silicalite.[20] The enthalpy of adsorption is smaller for pentane (23.4 $J \cdot g^{-1}$) than for hexane (27.4 $J \cdot g^{-1}$) or cyclohexane (25.9 $J \cdot g^{-1}$). Furthermore, the evaporation temperatures of the four solvents differ significantly: 36.2 °C for pentane, 68.0 °C for hexane, 80.7 °C for cyclohexane, and 98.0 °C for heptane. This might play an important role in the sample preparation, especially in the drying stage. A working hypothesis could be that pentane permits the creation of the smallest droplets of the salt solution. Then it has the smallest affinity for the silica surface and its evaporation temperature is low, so it evaporates quickly in the drying phase, leaving no traces. This is probably not the case for the other solvents which could have a negative? influence during the calcination stage. It could be imagined that traces of organic matter might act as reducing agents and introduce an unwanted reduction of cobalt.

However, to understand in more detail what happens at the surface during the "double solvent technique", we have searched for NMR and infrared data on the silica−solvent−water system. Despite numerous studies, there is not much information on the interaction between SBA-15 silica and alkane solvents, with water and with solvents and water. What happens structurally at the interface between SBA-15 and the liquids? Might there be a change in the hydrophilicity/hydrophobicity of the silica surface? Answers have been sought in a combined FT-IR, NMR (solid state ^{1}H-MAS, ^{29}Si -MAS, CP-MAS, and 2D CP-MAS-HETCOR), and microcalorimetry investigation.

Experimental Section

Synthesis. SBA-15 mesoporous silica was synthesized following the method by Choi et al.[21] This method employs milder acidic conditions than the synthesis by Zhao et al.,[1] which permits one to obtain larger yields that are, despite the batch size, homogeneous. A double-walled 2 L reactor with an integrated stirring rod enhanced the homogeneity of the texture. Aging occurred at 373 K during 20 h in closed containers. The as-synthesized silica was calcined at 773 K with a ramp of 2 $K \cdot min^{-1}$ and a dwell of 6 h. Part of the as-calcined SBA-15 silica was stocked in dry conditions, to avoid the adsorption of air moisture. Another part was immersed in water and dried overnight at 373 K. This is, what is called in this paper, hydroxylated SBA-15. Normapur alkane solvents were purchased from VWR: *n*-pentane (99% purity, max. 0.01% H_2O), *n*-heptane (99% purity, max. 0.0050% H_2O), and cyclohexane (99.5% purity, max. 0.01% H_2O). *n*-Heptane was purchased from Sigma Aldrich (99% purity and max. 0.001% H_2O). The solvents were used as received. The SBA-15 in solvent suspensions were made gravimetrically in a dry glovebox to avoid interaction with water in the air as much as possible.

Thermogravimetry and Differential Thermal Analysis (TG-DTA). TG-DTA analyses were performed on a Setaram setsys 16/18 apparatus. Samples of as-calcined and hydroxylated SBA-15 were heated to 1273 K, with a ramp of 5 $K \cdot min^{-1}$ under argon. The loss of chemisorbed water allowed the calculation of the number of OH groups at the surface.

FT-IR. The attenuated total reflection (ATR) mode of a Bruker Vertex 70 apparatus was used to measure FT-IR spectra in the wavenumber domain between 4000 and 400 cm^{-1}. A small quantity of powder was pressed on the diamond ATR crystal. In the case of a silica in alkane solvent suspension, a few droplets were pipetted onto the crystal and rapidly pressed before the solvent evaporated. Thirty-two scans were recorded. Deconvolution of the spectra was done with the aid of the OPUS software from Bruker Optics.

Solid State NMR. The solid state ^{1}H-MAS NMR, ^{29}Si-MAS NMR, ^{1}H-^{29}Si CP-MAS NMR, and the 2D ^{29}Si{^{1}H}-CP-HETCOR NMR spectra were recorded on a Bruker 400 Avance (9.40 T) spectrometer. A Bruker CP-MAS sonde was used with samples spinning at the magic angle at 5 kHz in 7 mm zirconia rotors. As a reference standard, tetramethylsilane (TMS) was used. To record the **^{1}H-**MAS NMR spectra, 16 acquisitions were collected with a 90° pulse of 4.85 μs and a recycle delay of 5 s. For the ^{29}Si-MAS NMR spectra, 32 or 288 experiments were recorded with a 90° pulse of 6 μs and a recycle delay of 200 s. The cross-polarization (CP) sequence used with 256 or 512 acquisitions was applied to record the ^{1}H-^{29}Si CP-MAS NMR spectra. The Hartmann−Hahn condition between ^{1}H and ^{29}Si was obtained using the transfer of a pulse of variable amplitude on the ^{1}H channel and a pulse of constant amplitude on the ^{29}Si channel. The contact time was 6 ms, the 90° pulse was 5 μs, and the recycle delay was 5 s with ^{1}H decoupling during the experiment. Also for the ^{29}Si{^{1}H} 2D heteronuclear correlation (HETCOR) experiments, a similar cross-polarization sequence was used, but now especially adapted for two dimensions. The contact time was 6 ms or 500 μs. The experiment was performed according to the States-TPPI method. The recycle time was 3 s, and the pulse duration was 5 μs (90°) with a ^{1}H decoupling during the acquisition. The spectra were deconvoluted using the DMFIT2004 software.[22]

Adsorption Studies. Nitrogen adsorption−desorption isotherms at 77 K were determined with a Micromeritics ASAP 2010 M apparatus. Before the experiment, the samples were heated for 4 h at 200 °C under a residual pressure lower than 200 Pa. Surface areas were determined by applying the BET equation and pore size distribution by the BJH method.[23,24] The adsorption−desorption isotherms of water on as-calcined and on a hydroxylated SBA-15 were determined by gravimetry with a homemade apparatus based on a symmetrical commercial vacuum microbalance from Setaram.[25] The adsorption isotherms of pentane and cyclohexane on as-calcined and hydroxylated SBA-15 and the corresponding enthalpies of adsorption were measured with a recently developed volumetric apparatus coupled with a microcalorimeter.[26] After being outgassed and heat-treated at 120 °C, the sample cell was placed inside the thermopile of a Tian-Calvet microcalorimeter and connected to a manifold. Due to a syringe and a homemade microleak-valve, the injection of liquid could be carried out either stepwise or continuously. The stepwise method was used in the present case. The amount adsorbed at a given pressure was obtained by measuring the difference to reach that pressure between the injected amount in the presence or absence of the sample. At each step, a calorimetric peak was recorded that allowed the corresponding adsorption enthalpy to be calculated.

Results and Discussion

Surface Structure of As-Calcined and Hydroxylated SBA-15 Silica. ***Water Sorption and DTA-TG Experiments.*** The adsorption and desorption isotherms of water vapor at as-calcined and hydroxylated SBA-15 have been recorded. The graph is shown in Figure 2. The first adsorption−desorption run gave rise to an isotherm of type V. The slope at the adsorption isotherm for as-calcined SBA-15 was very flat in

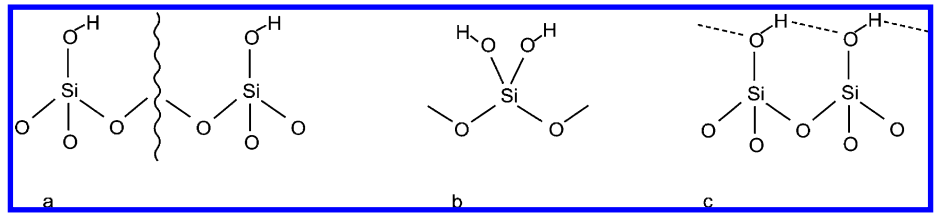

Figure 1. Proposed silanol groups at the silica surface: (a) isolated silanols, (b) geminal silanols, and (c) hydrogen-bonded silanols.

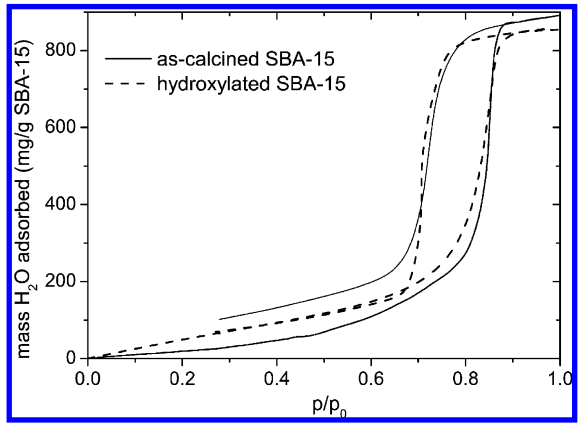

Figure 2. Adsorption and desorption isotherms of water vapor at as-calcined SBA-15 and hydroxylated SBA-15, measured at 298 K.

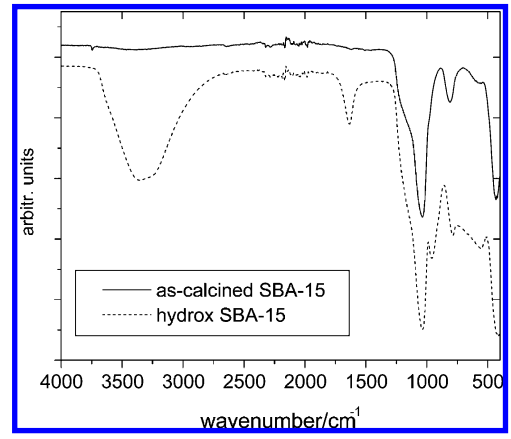

Figure 3. IR spectra in the range of 4000−400 cm^{-1} of as-calcined and hydroxylated SBA-15.

the low p/p_0 region, showing that as-calcined SBA-15 is rather hydrophobic. The sharp increase in the slope is the moment where the mesopores are getting filled. The hysteresis in the desorption isotherm is caused by the mesopores and is analogous with the result from a common nitrogen physisorption test, showing a similar hysteresis. However, in the desorption branch it is observed that it does not come back on the adsorption branch (no closure point). This means that water has been chemisorbed at the silica surface during the adsorption step, creating new silanol groups on the surface. Once rehydrated, a second run was performed. Now the isotherm became of type IV. This behavior confirms the findings on SBA-15 and other highly mesoporous silicas reported before.[27−31] It appeared that the adsorption and desorption isotherm are in equilibrium, implying that the silica surface is not reactive anymore with respect to water. The affinity of water for the rehydrated sample, as evidenced by the slope of the adsorption isotherm at the origin, is much higher than that for the as-calcined sample. The position of the plateau at saturation and of the steps of capillary condensation and evaporation are not affected by this rehydroxylation process. This is also the case for the adsorption isotherms of nitrogen on the same samples. It means that the SBA-15 sample is relatively stable toward water, opposite of MCM-41 type silicas that can show strong structural modifications by simple adsorption of water vapor.[32,33] These results indicate that during the two solvent procedure, rehydroxylation effects have to be considered. Additionally, it should be noted that several techniques exist to increase the stability of SBA-15 silicas, as summarized in ref 34. This includes, for example, synthesis under supercritical conditions or by microwave assistance, removing surface silanol groups, grafting heteroatoms, the use of preformed zeolite nanoclusters or seeds solution to assemble the walls, and increasing the degree of silica condensation.

The DTA-TG experiments showed that the loss of water until 423 K was negligible for as-calcined SBA-15 and 8 wt % for hydroxylated SBA-15. The loss of water between 423 and 1273 K was used to estimate the number of OH groups on the surface, because one can assume that in this temperature range, water loss corresponds mainly to condensation of silanols. Densification of the silica walls might also contribute to the amount of water, but at least as-calcined and hydroxylated silica can be compared in a relative way. Assuming that the OH groups are present as a monolayer and knowing that the average specific surface areas are 875 $m^2 \cdot g^{-1}$ for as-calcined SBA-15 and 800 $m^2 \cdot g^{-1}$ for hydroxylated SBA-15 (as deduced by N_2 adsorption measurements), the number of OH per nm^2 is 1.8 for as-calcined SBA-15, which is in agreement with values of 1.0−3.0 reported on several mesoporous silicas,[35−38] and 4.3 for hydroxylated SBA-15, which explains the more hydrophilic character of the latter.

Characterization by FT-IR Experiments. Figure 3 shows the FT-IR spectra of as-calcined and hydroxylated SBA-15. The differences are entirely due to the difference in the amount of water present in the system. In the as-calcined sample, the free silanol peak at 3746 cm^{-1} is observed (as in, e.g., refs 30, 37, and 39), which is gone in the case of hydroxylated SBA-15. The broad peak between 3700 and 3000 cm^{-1} in this spectrum is ascribed to the vibration bands of bonded OH groups. The peak at 1680 cm^{-1} is due to the presence of free water. The differences between as-calcined and hydroxylated silica in the 1200−500 cm^{-1} region (merely the domain of O−Si−O vibration bands) are caused by the introduction of Si−OH bending and stretching bands. The observed bands and to which modes of vibration they are attributed are listed in Table 1 for as-calcined SBA-15 and in Table 2 for hydroxylated SBA-15.

Characterization by ^{1}H-MAS and ^{29}Si-MAS Solid State NMR Experiments. Figure 4 shows the spectra of the ^{1}H-MAS NMR experiments on as-calcined and hydroxylated SBA-15. The observed peaks are listed in Table 4, with for each the chemical shift, the intensity, the peak width, the spin−spin relaxation time (T2) obtained by spin−echo measurements, and the integrated surface area under the peak. In the case of as-calcined silica, we can clearly distinct between several peaks that can be attributed to isolated, geminal, and hydrogen-bonded silanols at the surface. It has been experienced, however, that

TABLE 1: Observed Vibration Bands in As-Calcined SBA-15 and Their Assignments

wavenumber (cm^{-1})	nature of vibration
3746	νOH, stretching of isolated silanol
3734	νOH, stretching of geminal silanol
3700−3000[a]	stretching modes of bonded OH groups
1225	ν_aO−Si−O asymmetrical stretching
1150	ν_aO−Si−O asymmetrical stretching
1053	ν_aO−Si−O asymmetrical stretching
1020	ν_aO−Si−O asymmetrical stretching
975	νSi−OH stretching
955	unknown[b]
815	ν_aO−Si−O symmetrical stretching
795	δSi−OH bending
500−400[c]	rocking modes of the O−Si−O bond

[a] In this domain, three possibly distinguishable peaks are located at 3672, 3500, and 3250 cm^{-1}. [b] However, it is probably a Si−OH vibration. [c] Three major peaks are visible at, respectively, 460, 435, and 417 cm^{-1}.

TABLE 2: Observed Vibration Bands in Hydroxylated SBA-15 and Their Assignments

wavenumber (cm^{-1})	nature of vibration
3700−2500[a]	stretching modes of bonded OH groups
1640 and 1620	δH−O−H bending
1215	ν_aO−Si−O asymmetrical stretching
1135	ν_aO−Si−O asymmetrical stretching
1060	ν_aO−Si−O asymmetrical stretching
1025	ν_aO−Si−O asymmetrical stretching
962	νSi−OH, stretching of isolated silanol
918	δSi−OH···[OH_2][b]
807	ν_aO−Si−O symmetrical stretching
788	δSi−OH bending
650−500	wagging, rocking, and twisting modes of the H−O−H bond
500−400[c]	rocking modes of the O−Si−O bond

[a] Possibly distinguishable peaks are located at 3635, 3375, and 3230 cm^{-1}. [b] Tentatively assigned by the author. [c] Four peaks are distinguishable at, respectively, 468, 442, 424, and 411 cm^{-1}.

the spectrum taken from the same batch can differ from time to time, since dehydrated SBA-15 is very hydroscopic and the technique of ^{1}H-MAS NMR is very sensitive to the slightest trace of water.

What is known in literature about the different signals in a ^{1}H-MAS NMR spectrum of silica and how to attribute these to various chemical groups, such as free hydroxyls, or isolated silanols (Figure 1a), geminal silanols (Figure 1b), and hydrogen-bonded silanols (Figure 1c)? Heeribout et al.[40] performed ^{1}H-MAS NMR spectroscopy on amorphous silica. The major peaks found are located at 1.7, 2.9, and 3.7 ppm, which is interpreted as signals from, respectively, isolated silanol groups, hydrogen-bonded silanols, and adsorbed water. Shi et al.[41] have measured ^{1}H-MAS NMR spectra on SBA-15. Again three major peaks are found, and they propose the following: the 1.9 ppm peak is attributed to isolated silanol groups, 2.4 ppm to geminal silanols, and 3.0 ppm to hydrogenated silanols. Hommel et al. in ref 42 have studied the surface of nonporous vitreous silica and mention the following values: 2.2 ppm for isolated silanols and a shoulder between 3.3 and 3.8 ppm for geminal silanols. A possible peak for hydrogenated silanols at 3 ppm would fall in this zone. Paris et al.[43] have observed in amorphous opal a doublet at 0.9 and 1.3 ppm, which they ascribe to the existence of free hydroxyl groups. Hu et al.[44] have marked two peaks in calcined SBA-15: a narrow one at 1.61 ppm (isolated silanols) and a broader one at 3.5 ppm (combined contribution from both

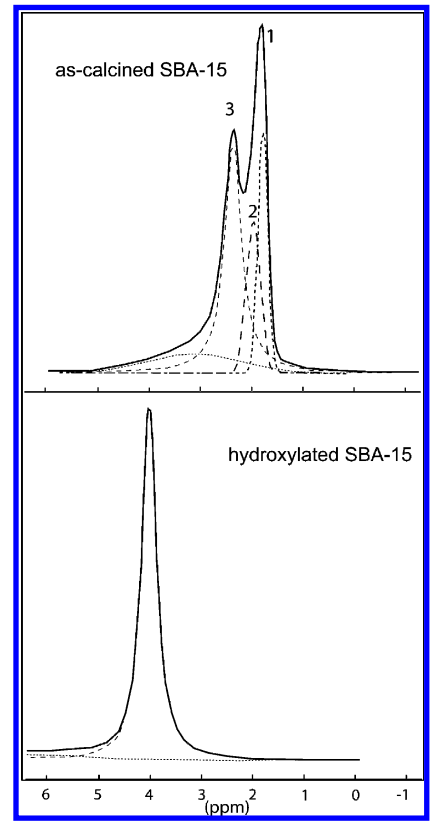

Figure 4. ^{1}H-MAS NMR spectra of as-calcined (above) and hydroxylated (below) SBA-15.

TABLE 3: Observed Vibration Bands in Alkane Solvents

wavenumber (cm^{-1})	nature of vibration
2960 and 2870	CH_3 stretching
2925 and 2850	CH_2 stretching
2890	CH stretching
1450 and 1380, 1360	CH_3 bending
1465	CH_2 bending
1340	CH bending
1260[a]	in *n*-alkanes and cyclohexane
1140	not present in cyclohexane
1040	only in cyclohexane
1020	not present in cyclohexane
1015	only in cyclohexane
920	not present in cyclohexane
910	not present in cyclohexane
900	only in cyclohexane
860	in *n*-alkanes and cyclohexane
800	in *n*-alkanes and cyclohexane
765	not present in cyclohexane
730	not present in cyclohexane
525	only in cyclohexane

[a] All peaks between 1260 and 730 cm^{-1} have been deconvoluted, since they interfere with the IR spectrum of silica. However, the exact assignment—probably C−C stretching and/or bending—of the nature of vibration cannot be made.

the silanol groups that are hydrogen bonded to water and water molecules that are hydrogen bonded to silanol groups) plus a shoulder extending from about 4.8 to 8 ppm. However, they have not deconvoluted their spectra, as the majority of the authors who have published on this subject. Baccile and Babonneau,[45] who have studied the spectra of grafted silica, found, among several peaks attributed to the grafted species, a broad peak at 5.5 ppm that was interpreted as a silanol group involved in hydrogen bonding with water molecules. Bae and

TABLE 4: Observed Peaks in the Solid State ^{1}H-MAS NMR Spectra

sample	pos (ppm)	I	fwhm (ppm)	T2 (ms)	% integral
as-cal SBA	1.8	13.6	0.23	3.42	19.9
	2.0	8.44	0.32	2.52	16.7
	2.4	12.8	0.41	1.93	48.8
	3.1	1.1	2.11	0.38	14.6
hydrox SBA	4.0	256	0.34	2.33	85.1
	5.5	3.5	1.58	0.50	5.4
	7.0	5.7	1.70	0.47	9.5
as-cal SBA + cyc	1.3	314	0.08	10.36	19.1
	1.4	980	0.11	7.25	78.7
	2.4	2.4	0.37	2.13	0.4
	2.8	9.4	0.22	3.63	1.4
	3.2	0.6	0.34	2.34	0.2
	3.7	0.6	0.66	1.21	0.2
as-cal SBA + pen	0.8	1738	0.11	7.25	53.0
	1.2	1470	0.11	7.25	43.2
	2.4	8.1	0.24	3.3	0.6
	2.5	3.8	0.18	4.53	0.2
	2.8	19.9	0.42	1.91	2.3
	3.3	2.1	0.68	1.17	0.3
	3.8	1.6	1.05	0.76	0.4
as-cal SBA + pen + H_2O	0.8	557	0.11	7.25	13.4
	1.2	494	0.13	6.04	14.3
	4.3	37.6	0.48	1.65	4.0
	4.7	1573	0.22	3.63	68.3
as-cal SBA + pen evap + H_2O	4.3	162	0.44	1.83	30.6
	4.7	756	0.21	3.76	69.4
hydrox SBA + pen	0.8	1467	0.09	9.07	37.2
	1.2	1134	0.11	7.25	35.9
	4.1	213	0.39	2.01	26.9

Han[46] found two peaks for calcined SBA-15: 1.5 and 3.5 ppm, interpreted as respectively isolated silanols and adsorbed water.

Based on these data, the following interpretation is proposed. The sharp peak at 1.8 ppm, which is indicated as peak number 1 in Figure 4, is attributed to the presence of isolated silanols. At 2.1 ppm (number 2), the peak for geminal silanols is found, and at 2.4 ppm (number 3) for hydrogen-bonded silanols. The evidence for the distinction between the two silanol types follows below. The presence of a monolayer of water is proposed to be marked by the presence of a broad peak at 3.1 ppm, while multilayers of water give rise to peaks at 4 ppm and higher. This is the case for hydroxylated SBA-15, as can be seen in the lower part of Figure 4, where only one peak can be distinguished, plus a tail from 5 ppm and higher.

In the ^{29}Si-MAS NMR spectra, shown in Figure 5, three peaks are present, at, respectively, ~−90, ~−100, and ~−110 ppm, classically attributed to Q_2, Q_3, and Q_4 sites (a.o.[35,42]). An overview of the observed peaks and their characteristics is given in Table 5. The qualitative, not quantitative, CP-MAS NMR spectra, which are not shown here, were used as an aid to interpret the peaks in the ^{29}Si-MAS NMR spectra, because the Q_3 and Q_2 peaks are more pronounced due to the magnetization transfer of the proton to the ^{29}Si nucleus. The major peak in both spectra is the one assigned to a Q_4 site. This means that the majority of the Si atoms are surrounded by four O−Si bonds and that apparently the major parts of the Si atoms are present in the walls of SBA-15, not at the surface. The amount of water in hydroxylated SBA-15 makes the difference in comparison with the as-calcined spectrum. The large number of water molecules create more Q_2 (geminal silanols) and Q_3 sites (isolated, but in the case of hydroxylated silica, especially H-bonded silanols) compared to dry SBA-15. Ratios of the surface areas of the peaks Q_2:Q_3, Q_2: Q_4, and Q_3:Q_4 are found in Table 6.

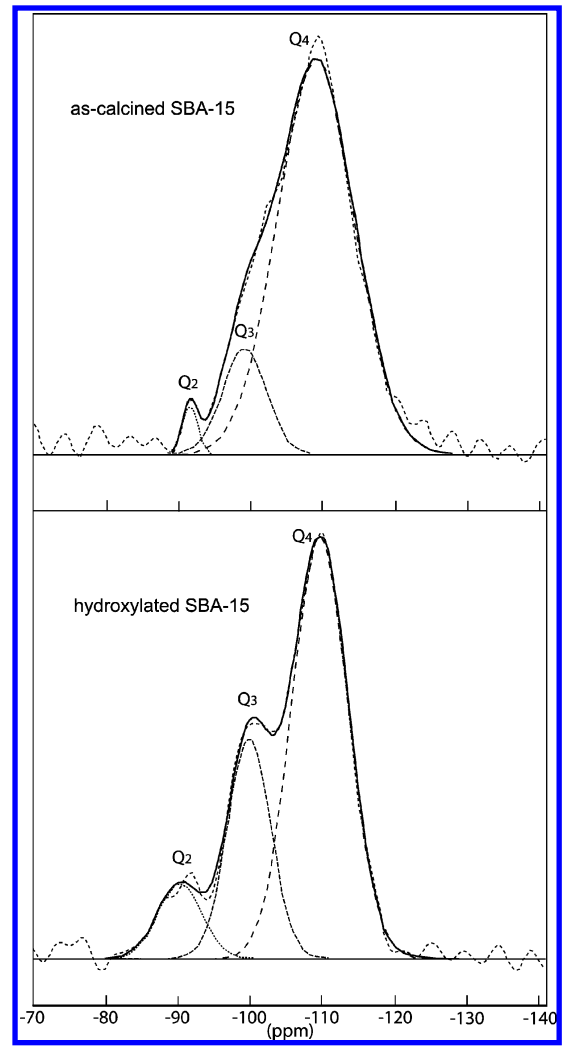

Figure 5. ^{29}Si MAS NMR spectra of as-calcined (above) and hydroxylated (below) SBA-15.

TABLE 5: Observed Peaks in the Solid State ^{29}Si-MAS NMR Spectra

sample	pos (ppm)	site	I	fwhm (ppm)	T2 (ms)	% integral
as-cal SBA	−91.7	Q_2	28	1.94	2.06	0.7
	−102.3	Q_3	194	11.5	0.35	28.7
	−110.6	Q_4	496	10.61	0.38	70.6
hydrox SBA	−90.4	Q_2	11	7.19	0.56	9.0
	−99.9	Q_3	31	7.01	0.57	26.0
	−109.7	Q_4	60	9.16	0.44	65.0
as-cal SBA + cyc	−90.1	Q_2	11	3.22	1.24	0.6
	−101.7	Q_3	188	10.53	0.38	32.0
	−110.0	Q_4	427	10.17	0.39	67.4
as-cal SBA + pen	−92.3	Q_2	27	5.92	0.68	3.1
	−100.3	Q_3	121	7.19	0.56	17.0
	−109.2	Q_4	384	11.15	0.36	79.9
as-cal SBA + pen, evap	−90.9	Q_2	5	2.35	1.71	1.2
	−100.9	Q_3	22	7.27	0.55	15.7
	−109.6	Q_4	69	10.97	0.37	83.1

Assuming that the 1.8 ppm peak in the ^{1}H-MAS NMR spectrum for as-calcined SBA-15 corresponds to the isolated silanols, there remains possibly the question how to distinguish between the geminal and H-bonded silanol types. The evidence comes from the 2D-HETCOR NMR spectrum of as-calcined SBA-15, which is shown in Figure 11. The correlation spot between the Q_2 peak in the ^{1}H >^{29}Si-CP-MAS NMR spectrum (x-axis) and the ^{1}H spectrum (y-axis) falls slightly under the

TABLE 6: Peak Ratios in the Solid State ^{29}Si-MAS NMR Spectra

sample	Q2:Q4	Q3:Q4	Q2:Q3
as-cal SBA	0.010	0.406	0.024
hydrox SBA	0.139	0.399	0.347
as-cal SBA + cyc	0.009	0.476	0.018
as-cal SBA + pen	0.039	0.213	0.1823
as-cal SBA + pen, evap	0.015	0.189	0.078

spot between the Q_3 peak and the ^{1}H spectrum. In fact, the latter correlation is centered around 1.8 ppm on the *y*-axis, while the former is centered at 2.1 ppm. So the fact that the strongest correlation exists between the Q_2 site and the peak at 2.1 ppm in the ^{1}H-MAS NMR spectrum leads to the conclusion that this peak is probably attributable to the presence of geminal silanols. As a result, the rather sharp peak at 2.4 ppm is therefore assigned to H-bonded silanols.

According to the amount of water present in a "dry" SBA-15 sample, the shoulder at 2.4−3 ppm is more or less pronounced. In the case of hydroxylated silica, the "excess" of water covers all peaks due to subtle interactions; the peak at 4 ppm is due to the presence of (multi)layers of adsorbed water.

Surface Structure of As-Calcined and Hydroxylated SBA-15 Silica in the Presence of Alkane Solvents. When carrying out both the FT-IR and NMR experiments, it has been observed that the subtle interactions between the silica surface and alkane solvents are only well visible in the case of a dehydrated surface. As soon as some water is present, this covers the interactions entirely, and only vibrations due to water are measured. This was a reason to work with only dry, as-calcined SBA-15 when doing the tests on mixtures of SBA-15 and alkanes. The focus has been placed on *n*-pentane and cyclohexane, since they gave the most extreme results in a previous study, where we loaded SBA-15 with cobalt oxide nanoparticles,[16] a pentane treatment leading to finely dispersed small nanoaggregates, while cyclohexane gave rise to large, heterogeneously distributed aggregates of cobalt oxide.

Characterization by FT-IR Experiments. Before the FT-IR tests were performed on mixtures of SBA-15 with the alkane solvents, the solvents have been recorded to prove they were absolutely dry, which was the case. The observed vibration bands are tabulated in Table 3. In the FT-IR spectra recorded on mixtures of dry SBA-15 with an alkane solvent, of which the plots are shown in Figure 6 and Figure 7, a few phenomena

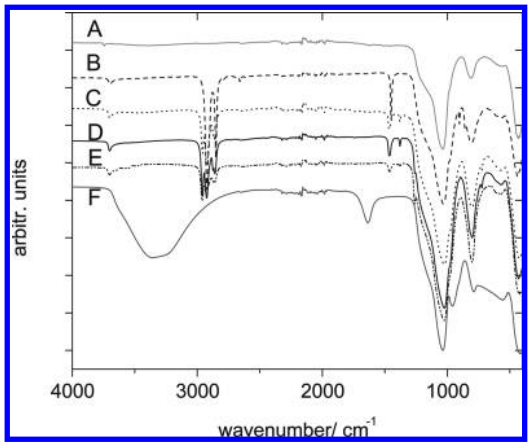

Figure 6. IR spectra in the range of 4000−400 cm^{-1}: (A) as-calcined SBA-15, (B) as-cal SBA-15 + cyclohexane, (C) as-cal SBA-15 + heptane, (D) as-cal SBA-15 + hexane, (E) as-cal SBA-15 + pentane, and (F) hydroxylated SBA-15.

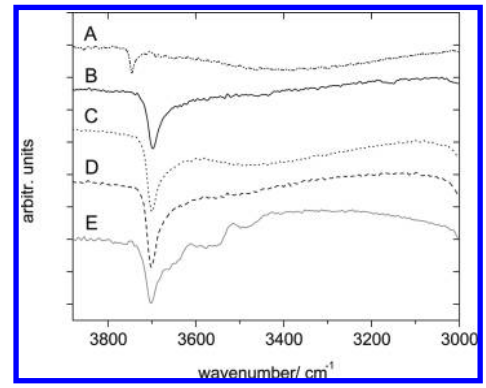

Figure 7. Close-up of the IR spectra in the range of 3850−3100 cm^{-1}, to show the shift of the peak that is assigned to free hydroxyls. The legend is the same as in Figure 6, except for hydroxylated SBA-15, which is not shown.

were observed that were valid for all four solvents: pentane, hexane, heptane, and cyclohexane. A shift of the free silanol peak at 3746 cm^{-1} toward 3700 cm^{-1} is noted, which has been also observed for other solvents, such as CCl_4.[47] This red shift is caused by the interaction of the surface hydroxyls with the surrounding molecules. For all our four tested solvents, the same effect was observed. With pentane only, several additional broad peaks around 3500 cm^{-1} are observed. These peaks are difficult to interpret with the present data, but one could think of the formation of carboxylic groups, by reaction between pentane and some acidic sites in the SBA-15. Furthermore, an increase in the shoulder at 3690 cm^{-1} compared to the 3700 cm^{-1} peak is observed, which is not the case for the peak in the mixtures with the other three solvents (Figure 7). This shoulder has been ascribed to geminal silanols.[48] This would imply that wetting with pentane instead of another solvent would cause an increase in the number of geminal silanols compared to isolated silanols.

Studying carefully the spectrum of as-calcined SBA-15, it can be seen that the part between 3500 and 3000 cm^{-1}, the zone where the broad peak is present in the hydroxylated SBA-15 sample, is not entirely flat. Moreover, there is a hint of a peak at 1680 cm^{-1}—where a clear peak is present in hydroxylated silica. The vibration bands that make up the zone between 3500 and 3000 cm^{-1} are assigned to bonded OH groups. The 1680 cm^{-1} peak is that of free water. This means that our calcined sample contains water. An interesting effect of adding a solvent is that both the bulge and the peak at 1680 cm^{-1} have disappeared. It seems that the solvent removes the traces of water, while rehydroxylating the silica surface. How can we envision the interaction between the alkane solvent and the silica surface? It is known that pentane is a weak proton donor.[49] At the same time it has been shown that silanol groups at the silica surface are not Brønsted acidic.[50] This would suggest the tendency to accept protons and to create weak H bonds with pentane.

Evidence by ^{1}H-MAS and ^{29}Si-MAS Solid State NMR Experiments. As was done before performing the IR experiments, the solvents that were used were tested by ^{1}H-MAS NMR, to show that they did not contain water.

The ^{1}H-MAS NMR spectra of as-calcined SBA-15 plus pentane and, respectively, cyclohexane have been recorded, which can be found in Figure 8. The observed peaks are listed in Table 4. The main effect observed in these spectra is the disappearance of the peak that is characteristic for isolated silanol. Moreover, two peaks appear that could be ascribed to respectively geminal and hydrogenated silanols.

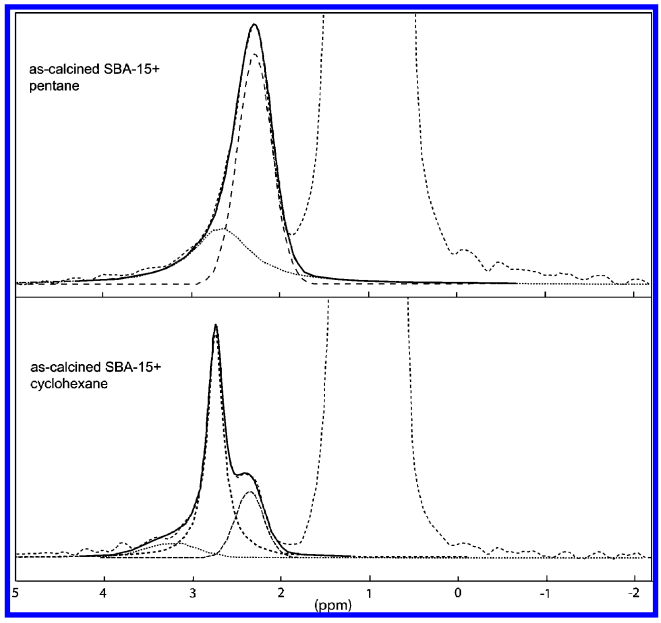

Figure 8. ^{1}H-MAS NMR spectra of as-calcined SBA-15 plus pentane in a molar ratio of 1.0 SBA-15:0.8 pentane (above) and as-calcined SBA-15 plus cyclohexane in a molar ratio of 1.0 SBA-15:0.8 cyclohexane (below).

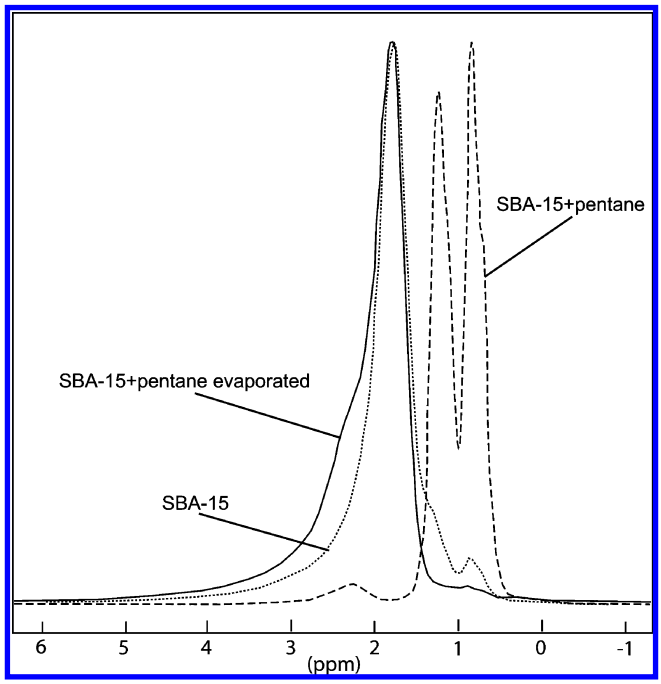

Figure 9. ^{1}H-MAS NMR spectra of as-calcined SBA-15, as-calcined SBA-15 with pentane, in a molar ratio of 1.0 SBA-15:0.8 pentane, and as-calcined SBA-15 that was in contact with pentane, where pentane was evaporated. The spectra are normalized to the peak maxima.

A test was performed on the reversibility of this effect with as-calcined SBA-15 and pentane only. After evaporation of the pentane that was in contact with the SBA-15, again a ^{1}H-MAS NMR spectrum was recorded. It appeared that the peak shift was not completely reversible. In the evaporated sample, the peak that we attribute to geminal silanols was larger compared to the pure SBA-15 sample, and the peak ascribed to hydrogenated silanols was there permanently; see Figure 9. It seems that pentane modifies slightly the silica surface. In addition, a test was done to see whether it would make a difference to evaporate the pentane before adding the aqueous solution

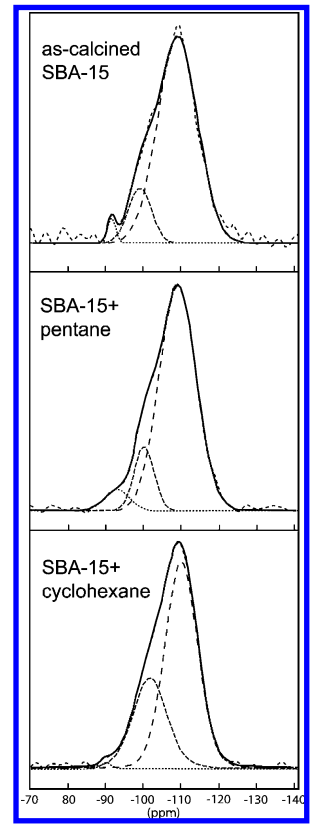

Figure 10. ^{29}Si-MAS NMR spectra of as-calcined SBA-15 (above), as-calcined SBA-15 plus pentane in a molar ratio of 1.0 SBA-15:0.8 pentane (middle), and as-calcined SBA-15 plus cyclohexane in a molar ratio of 1.0 SBA-15:0.8 cyclohexane.

(=H_2O). This was not the case, as can be seen from the peak parameters in Table 4.

The ^{29}Si-MAS NMR spectra in Figure 10 show that there is an increase of Q_2 sites in as-calcined SBA-15 when mixed with pentane (in a 1 SBA-15:0.8 pentane ratio), compared to as-calcined SBA-15. This is, however, not the case for as-calcined SBA-15 in the presence of cyclohexane. What the spectra are showing is also quantified by the Q_2:Q_4 ratios that are found in Table 6. The Q_2:Q_4 ratio for as-calcined SBA-15 and as-calcined SBA-15 in contact with cyclohexane is 0.010 and 0.009, respectively. This ratio is significantly higher for as-calcined SBA-15 with pentane. This implies that pentane indeed modifies the silica surface, creating more geminal silanol sites.

Hypothesis on the Double Solvent Technique. It should be noted that the aim of this study was not to optimize the pore loading, but principally to understand what we have observed in the previous study. The hypothesis we propose on the interactions that take place while carrying out the double solvent technique is the following. When a solvent is entering the pore system, traces of water that are present are pushed against the silica wall, causing a rehydroxylation of the surface. This results in a more hydrophilic behavior of the surface, which might favor the interaction with an aqueous solution that is introduced afterward. In the next stage, where an aqueous solution is introduced, droplets of the solution are formed in the alkane solvent. Since the interfacial tension between pentane and water is smaller compared to the other alkanes we have studied, as is discussed in the Introduction, it is expected that in pentane the smallest droplets are formed, which would enhance the dispersion on the SBA-15 pore system. In the drying stage, it is important to remove all traces of solvent left. It can be imagined that, if some solvent molecules stay in the pores, those might

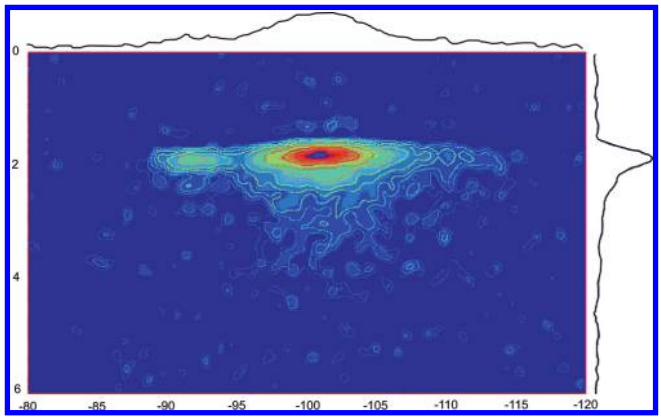

Figure 11. 2D HETCOR NMR spectrum of as-calcined SBA-15.

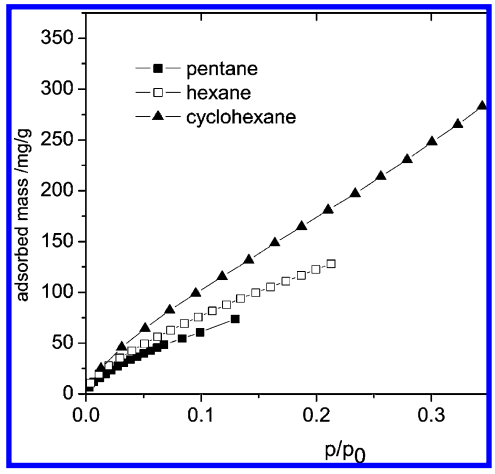

Figure 12. Adsorption isotherms of pentane, hexane, and cyclohexane on hydroxylated SBA-15.

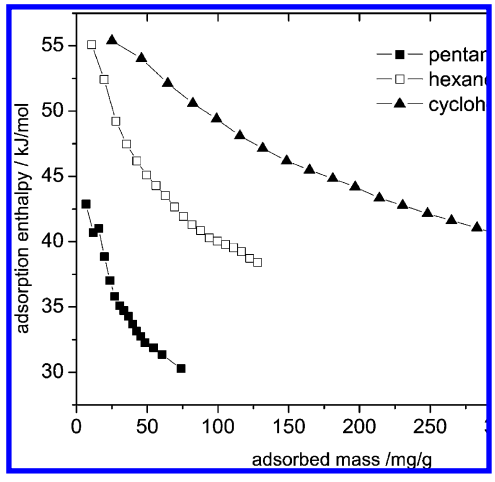

Figure 13. Adsorption enthalpies of pentane, hexane, and cyclohexane on hydroxylated SBA-15.

hinder during the calcination step. It is known that the enthalpy of adsorption for pentane on a massive silica surface is the smallest compared to the higher alkanes. That this is also the case for SBA-15 silica has been confirmed by microcalorimetry experiments. The results for pentane, hexane, and cyclohexane are shown in Figure 12 and Figure 13. The adsorption isotherm of heptane at room temperature as reported by ref 51 fits in the trend shown here. Our experiments evidenced the smallest affinity for pentane on a SBA-15 surface. This would imply that it is easier to remove, which is also facilitated by its low evaporation temperature. So the phenomena observed by IR and NMR spectroscopy, completed by calorimetry and literature data, can explain that a treatment with pentane is favorable compared to another alkane solvent, in order to obtain finely dispersed nanoaggregates of metal oxides.

Conclusions

This work has been carried out to find an explanation of the mechanisms of the so-called double solvent technique, a way to impregnate mesoporous silica with a metal oxide precursor using an alkane solvent as a prewetting agent. This technique has been simulated during IR and NMR experiments. A slight silica surface modification has been observed when adding an alkane. The majority of the surface groups of dry SBA-15 are isolated silanols, next to a smaller part that consists of geminal and hydrogen-bonded silanols. The addition of an alkane seems to cause an increase in the number of geminal and hydrogen-bonded silanol groups, which is augmenting the hydrophilic nature of the silica. Based on data from microcalorimetry measurements of the adsorption enthalpy and data from literature on the interfacial tension between water and alkanes, which follow the same trend, we can propose a hypothesis as to why the prewetting with an alkane solvent, and especially pentane, improves the dispersion of cobalt oxide nanoparticles in the pores of SBA-15. In the Introduction, we have mentioned the possible application of this technique to the encapsulating of radioactive chloride salts in SBA-15. Tests with neodymium chloride salts show that it is possible to introduce them in the pores in a similar way. First essays have been carried out on an in situ oxidation of the chloride salt, since this will render it less soluble. However, more research is needed to improve the fixation.

References and Notes

(1) Zhao, D.; Feng, J.; Huo, Q.; Melosh, N.; Frederickson, G. H.; Chmelka, B. F.; Stucky, G. D. *Science* **1998**, *279*, 548–552.
(2) Sayari, A. *Chem. Mater.* **1996**, *8*, 1840–1852.
(3) Galarneau, A.; Desplantier-Giscard, D.; DiRenzo, F.; Fajula, F. *Catal. Today* **2001**, *68*, 191–200.
(4) Ressler, T.; Walter, A.; Huang, Z.-D.; Bensch, W. *J. Catal.* **2008**, *254*, 170–179.
(5) Dai, Z.; Bao, J.; Yang, X.; Ju, H. *Biosens. Bioelectron.* **2008**, *23*, 1070–1076.
(6) Liu, Y.; Zhang, J.; Hou, W.; Zhu, J.-J. *Nanotechnology* **2008**, *19*, 135707 (8 pp).
(7) Manzanoa, M.; Aina, V.; Aréan, C.; Balas, F.; Cauda, V.; Colilla, M.; Delgado, M. R.; Vallet-Regí, M. *Chem. Eng. J.* **2008**, *137*, 30–37.
(8) Mellaerts, R.; Mols, R.; Jammaer, J. A. G.; Aerts, C. A.; Annaert, P.; van Humbeeck, J.; van den Mooter, G.; Augustijns, P.; Martens, J. A. *Eur. J. Pharm. Biopharm.* **2008**, *69*, 223–230.
(9) *Chemical Separation Technologies and Related Methods of Nuclear Waste Management*; Choppin, G. R., Khankhasayev, M. K., Eds.; Kluwer Academic Publishers: Dordrecht, Netherlands, 1998.
(10) Impéror-Clerc, M.; Bazin, D.; Appay, M.-D.; Beaunier, P.; Davidson, A. *Chem. Mater.* **2004**, *16*, 1813–1821.
(11) Bezemer, G. L.; Bitter, J. H.; Kuipers, H. P. C. E.; Oosterbeek, H.; Holewijn, J. E.; Xu, X.; Kapteijn, F.; van Dillen, A. J.; de Jong, K. P. *J. Am. Chem. Soc.* **2006**, *128*, 3956–3964.
(12) Lopes, I.; Hassan, N. E.; Guerba, H.; Wallez, G.; Davidson, A. *Chem. Mater.* **2006**, *18*, 5826–5828.
(13) Vrålstad, T.; Glomm, W. R.; Rønning, M.; Dalthe, H.; Jentys, A.; Lercher, J. A.; Øye, G.; Stöcker, M.; Sjöblom, J. *J. Phys. Chem. B.* **2006**, *110*, 5386.
(14) Salabas, E.-L.; Rumplecker, A.; Kleitz, F.; Radu, F.; Schüth, F. *Nano Lett.* **2006**, *6*, 2977–2981.
(15) Sietsma, J. R. A.; Meeldijk, J. D.; den Breejen, J. P.; Versluis-Helder, M.; van Dillen, A. J.; de Jongh, P. E.; de Jong, K. P. *Angew. Chem., Int. Ed.* **2007**, *46*, 4547–4549.
(16) Van der Meer, J.; Bardez, I.; Bart, F.; Albouy, P.-A.; Wallez, G.; Davidson, A. *Microporous Mesoporous Mater.* **2009**, *118*, 183–188.
(17) Matsubara, H.; Murase, M.; Mori, Y. H.; Nagashima, A. *Int. J. Thermophys.* **1988**, *9*, 409–424.
(18) Zeppieri, S.; Rodríguez, J.; de Ramos, A. L. L. *J. Chem. Eng. Data* **2001**, *46*, 1086–1088.

(19) Matthews, J. B. *Trans. Faraday Soc.* **1939**, *35*, 1113–1122.
(20) Blum, Z.; Hyde, S. T.; Ninham, B. W. *J. Phys. Chem.* **1993**, *97*, 661–665.
(21) Choi, M.; Heo, W.; Kleitz, F.; Ryoo, R. *Chem. Commun.* **2003**, 1340–1341.
(22) Massiot, D.; Fayon, F.; Capron, M.; King, I.; Calvé, S. L.; Alonso, B.; Durand, J.-O.; Bujoli, B.; Gan, Z.; Hoatson, G. *Magn. Reson. Chem.* **2002**, *40*, 70–76.
(23) Barrett, E. P.; Joyner, L. G.; Halenda, P. P. *J. Am. Chem. Soc.* **1951**, *73*, 373–380.
(24) Rouquerol, F.; Rouquerol, J.; Sing, K. S. W. *Adsorption by Powders and Porous Solids*; Academic Press, London: 1999.
(25) Rouquerol, J.; Davy, L. *Thermochim. Acta* **1978**, *24*, 391.
(26) Denoyel, R.; Beurroies, I.; Vincent, D. *J. Therm. Anal. Cal.* **2002**, *70*, 483–492.
(27) Inagaki, S.; Fukushima, Y.; Kuroda, K.; Kuroda, K. *J. Colloid Interface Sci.* **1996**, *180*, 623–624.
(28) Takahara, S.; Nakano, M.; Kittaka, S.; Kuroda, Y.; Mori, T.; Hamano, H.; Yamaguchi, T. *J. Phys. Chem. B* **1999**, 5814–5819.
(29) Matsumoto, A.; Tsutsumi, K.; Schumacher, K.; Unger, K. K. *Langmuir* **2002**, *18*, 4014–4019.
(30) Matsumoto, A.; Sasaki, T.; Nishimiya, N.; Tsutsumi, K. *Colloids Surf., A* **2002**, *203*, 185–193.
(31) Morishige, K.; Kanzaki, Y. *J. Phys. Chem. C* **2009**, *113*, 14927–14934.
(32) Iapichella, J.; Meneses, J.-M.; Beurroies, I.; Denoyel, R.; Bayram-Hahn, Z.; Unger, K.; Galarneau, A. *Microporous Mesoporous Mater.* **2007**, *102*, 111–121.
(33) Carrott, M. M. L. R.; Candeias, A. J. E.; Carrott, P. J. M.; Unger, K. K. *Langmuir* **1999**, *15*, 8895–8901.
(34) Du, Y.; Lan, X.; Liu, S.; Ji, Y.; Zhang, Y.; Zhang, W.; Xiao, F.-S. *Microporous Mesoporous Mater.* **2008**, *112*, 225–234.
(35) Zhao, X. S.; Lu, G. Q.; Whittaker, A. K.; Millar, G. J.; Zhu, H. Y. *J. Phys. Chem. B* **1997**, *101*, 6525–6531.
(36) Widenmeyer, M.; Anwander, R. *Chem. Mater.* **2002**, *14*, 1827–1831.
(37) Jarupatrakorn, J.; Tilley, T. D. *J. Am. Chem. Soc.* **2002**, *124*, 8380–8388.
(38) Nozaki, C.; Lugmair, C. G.; Bell, A. T.; Tilley, T. D. *J. Am. Chem. Soc.* **2002**, *124*, 13194–13203.
(39) Landmesser, H.; Kosslick, H.; Storek, W.; Fricke, R. *Solid State Ionics* **1997**, *101*−*103*, 271–277.
(40) Heeribout, L.; d'Espinose de la Caillerie, J. B.; Legrand, A. P.; Mignani, G. *J. Colloid Interface Sci.* **1999**, *215*, 296–299.
(41) Shi, L.; Zou, Y.; He, H. *Chem. Lett.* **2001**, 1164–1165.
(42) *The Surface Properties of Silica*; Legrand, A. P. , Ed.; Wiley: Chichester, U.K., 1998.
(43) Paris, M.; Fritsch, E.; Reyes, B. O. A. *J. Non-Cryst. Solids* **2007**, *353*, 1650–1656.
(44) Hu, J. Z.; Kwak, J. H.; Herrera, J. E.; Wang, Y.; Peden, C. H. F. *Solid State NMR* **2005**, *27*, 200–205.
(45) Baccile, N.; Babonneau, F. *Microporous Mesoporous Mater.* **2008**, *110*, 534–542.
(46) Bae, Y. K.; Han, O. H. *Microporous Mesoporous Mater.* **2007**, *106*, 304–307.
(47) Heilweil, E. J.; Casassa, M. P.; Cavanagh, R. R.; Stephenson, J. C. *J. Chem. Phys.* **1985**, *82*, 5216–5231.
(48) Diaz, L.; Liauw, C. M.; Edge, M.; Allen, N. S.; McMahon, A.; Rhodes, N. *J. Colloid Interface Sci.* **2005**, *287*, 379–387.
(49) Jalilian, M. R. *Spectrochim. Acta* **2007**, *A 66*, 91–93.
(50) Landmesser, H.; Kosslick, H.; Kürschner, U.; Fricke, R. *J. Chem. Soc., Faraday Trans.* **1998**, *94*, 971–977.
(51) Hoang, V.-T.; Huang, Q.; Eić, M.; Do, T.-O.; Kaliaguine, S. *Langmuir* **2005**, *21*, 5094–5101.

JP907002Y